POLITECNICO DI TORINO
Repository ISTITUZIONALE

Two-Phase flow instrumentation for nuclear accidents simulation, Keynote lecture KN3, pp. 1-23, Procs. 32nd UIT Heat Transfer Conference, Pisa, June 23-25, 2014.

Original
Two-Phase flow instrumentation for nuclear accidents simulation, Keynote lecture KN3, pp. 1-23, Procs. 32nd UIT Heat Transfer Conference, Pisa, June 23-25, 2014 / Monni, Grazia; DE SALVE, Mario; Panella, Bruno. - ELETTRONICO. - Unico-Keynote lecture KN3:(2014), pp. 1-23. (Intervento presentato al convegno 32nd UIT Heat Transfer Conference tenutosi a Pisa nel 23-26 June 2014).

Availability:
This version is available at: 11583/2565551 since:

Publisher:
Università di Pisa

Published
DOI:

Terms of use:

This article is made available under terms and conditions as specified in the corresponding bibliographic description in the repository

Publisher copyright

(Article begins on next page)

30 November 2023

Two-Phase flow instrumentation for nuclear accidents simulation

G Monni, M De Salve and B Panella
Energy Department, Politecnico di Torino, Corso Duca degli Abruzzi, 24, 10129 Torino, Italy

E-Mail: bruno.panella@polito.it

Abstract
The paper presents the research work performed at the Energy Department of the Politecnico di Torino, concerning the development of two-phase flow instrumentation and of models, based on the analysis of experimental data, that are able to interpret the measurement signals. The study has been performed with particular reference to the design of power plants, such as nuclear water reactors, where the two-phase flow thermal fluid dynamics must be accurately modeled and predicted. In two-phase flow typically a set of different measurement instruments (Spool Piece - SP) must be installed in order to evaluate the mass flow rate of the phases in a large range of flow conditions (flow patterns, pressures and temperatures); moreover, an interpretative model of the SP need to be developed and experimentally verified. The investigated meters are: Turbine, Venturi, Impedance Probes, Concave sensors, Wire mesh sensor, Electrical Capacitance Probe. Different instrument combinations have been tested, and the performance of each one has been analyzed.

1. Introduction

The design of power plants, involving two-phase flow, such as nuclear water reactors, requires the ability to model and predict the flow thermal fluid dynamics, with a required degree of accuracy, while on the other hand accurate experimental data need to be used in order to validate the simulation tools usually adopted during the design phase. For example, the design of nuclear reactors requires to carry out integral tests, used to simulate the thermo-hydraulics of a PWR in a scaled-down test facility and for safety codes validation (like RELAP and TRAC), and separate effect tests, where the local phenomena of the flow are investigated using sensor characterized by a sufficiently high time and space resolution.

Due to the complex nature of the two-phase flow, the measurement of the flow parameters, such us phases distribution, velocities, interfaces evolution, require the application of special instrumentation an d the development of interpretative models of the experimental signals based on both the physics of the sensor and of the flow. Successful application of a measuring system/ device in a two-phase test facility does not guarantee its applicability in every flow or loop conditions. Intrusive and nonintrusive measurement techniques of two-phase flows, with special application to the determination of mass flow rates, have been developed, in particular to investigate Design Basis Accidents like loss of coolant accidents (LOCA), where the measurement of the mass flow rate of the two phases was required to analyze the accident evolution. Nowadays new experimental campaigns are required for the licensing of the new advanced reactors, like the Small Modular Reactors, so that the development of reliable instruments is required for the measurement of the fundamental parameters of the flow, under as many as possible two-phase flow conditions. As an example, the SPES3 experimental facility [1], able to simulate the innovative small and medium size PWR nuclear reactors, is being built and will be operated by the SIET Company.

An accurate accident analysis requires the measurement of the mixture mass flow rate and instruments and methodologies to evaluate different two-phase flow parameters have to be developed. Typically a set of different measurement instruments (Spool Piece - SP) must be installed in order to evaluate the mass flow rate of the phases and a model of the SP, depending on the geometry and on the SP orientation, is required. The selection of the instruments strongly depends on the experimental

conditions: pressure, temperature and phases velocities. In the present paper the experimental result and the models developed for different instruments and different SP is presented. Based on a bibliographic analysis of the available instruments, suitable to be installed in the SPES3 simulation facility [2], a number of instruments have been experimentally and theoretically studied: Turbine [3], Drag disk [3], Venturi [4], Impedance Probes, Concave sensors, Wire mesh sensor (WMS) [5], Electrical Capacitance Probe (ECP) [6], designed by SIET S.P.A. Their measurement characteristics have been investigated, taking in account the range of measurement, dynamic response, installation requirements, materials/electrical compatibility with pressure and temperature conditions, flow velocity compatibility. The selected devices can operate in the whole range of conditions expected in the break lines of the experimental facility: void fractions (from 0 to 1), pressure (up to 155 bar), temperature (higher than 200°C), velocity (gas velocity up to 200 m/s). Moreover the flow pattern is likely to be also time dependent and the measurement is complicated by the fact that during the transient the fluid becomes a non homogeneous mixture of water and steam.

Different instrument combinations have been tested, with air and water at low pressure and temperature, and the performance of each one has been analyzed in terms of estimation of the mass flow rate of the two phases, identifying their advantage and drawbacks, and estimating the phases mass flow rate measurement accuracy for each SP configuration. All details, concerning the two-phase flow instrumentation and the general criteria for the instruments selection, can be found in ref. [7].

2. Two-Phase Flow Investigation with WMS

The Wire-Mesh Sensors (WMS), based on the measurement of the local instantaneous conductivity of the two-phase mixture, are used for a high-speed visualization of a gas–liquid flow as well as for the measurement of void fraction profiles, bubble size distributions and gas velocity distributions [8,9,10]. The WMS, able to measure directly the conductivity between pairs of crossing wires, can be used to detect the presence of the phases in the different measuring points, and allows an high space and time resolution. In the present work, the WMS has been used to investigate the air-water flow in a horizontal Plexiglas pipeline (inner diameter D=19.5 mm), for several flow patterns. The local, chordal, cross-sectional void fraction are estimated from the sensor data. The flow evolution in time and space is analyzed and the characteristics for all the flow patterns are derived by means of a statistical analysis. The adopted sensor (Fig. 1) has been manufactured by Teletronic Rossendorf GmbH [11]. It consists of two planes of parallel wire grids (16x16) that are placed across the channel at a short distance from each other (1.5 mm); the wires of both planes cross under an angle of 90°. The sensor has been designed to cover the cross section of a channel having a 19.5 mm inner diameter; the wires have a diameter D_{wire} of 70 μm and a pitch p equal to 1.3 mm, so only the 5.4% of the pipe section is occupied by the sensor.

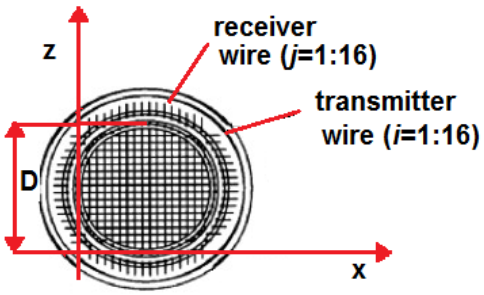

Fig. 1. Scheme of the WMS.

The measuring grid allows a spatial resolution of the order of the pitch length (1.3 mm), that combined with the high time resolution (up to 10.000 frames/s) allow the investigation of the local phenomena of the flow and their time evololution. The output is a 3-D matrix $V^*(i,j,k)$, where the indexes i and j are related to the space position of the mesh points and k is the time index, having a value between 1 and $T_T \cdot f_{acq}$, where T_T is the total observation time and f_{acq} is the acquisition frequency. The indexes i and j refer to transmitting wires and to receiving wires respectively. The developed signal processing scheme is structured to obtain the desired two-phase flow parameters. First of all the signal is normalized taking into account the single phase reference matrices, $V_g(i,j)$ and $V_l(i,j)$:

$$V^*(i,j,k) = \frac{V(i,j,k) - V_l(i,j)}{V_g(i,j) - V_l(i,j)} \tag{1}$$

The signal normalization can be considered as an approximation of the local void fraction value, if a linear relationship between conductivity and void fraction and a reference area equal to the square of the wire pitch p are assumed. From the evaluated local void fraction, the instantaneous chordal profiles are derived. The vertical profiles in the centre line of the pipe (index j=8) are used to evaluate the characteristic times and the characteristic shape of the void fraction profiles for the different flow conditions. The local instantaneous void fraction α has been obtained with an acquisition frequency f_{acq} equal to 1250 Hz for a total observation time T_T equal to 20 s. Further details can be found in ref. [12]. The local void fraction in each point of the sensor grid is characterized by the signal histogram: the analysis of the normalized histograms, that are evaluated for the total observation time, allows us to define if a deterministic or a stochastic behavior characterizes the flow. The parameter σ/α_{mean}, where σ is the standard deviation of the signal and α_{mean} is the average void fraction is used as an index of the fluctuation of the signal. For non intermittent flows, the standard deviation value of the local void fraction is small, and the flow can be characterized with well defined void fraction profiles. If the probability density function PDF is not a Gaussian curve and a quasi periodic behavior can be defined for the macroscopic structures of the flow, the characteristic times and the characteristic profiles have to be derived. In order to analyze fast phenomena in terms of average values, a moving average of the void fraction time values has been performed using a time interval τ. Once the averaging time interval is defined, every average profile has been characterized from the statistical point of view by the root mean square profiles; while the variation in time of the chordal profile has been analyzed considering the evolution of the parameter $M(t)$ defined as the sum along the chord of the difference between the moving average local void fraction evaluated at the time t and at the time t-Δt:

$$M(t) = \sum_{i=1}^{16} \left(< \alpha(i,j,t) > - < \alpha(i,j,t-\Delta t) > \right) \tag{2}$$

t is equal to k / f_{aca} and Δt is equal to $1/f_{aca}$. Starting from the evolution in time of the $M(t)$ parameter it is possible to define the time interval in which the profile is constant and the time interval in which is evolving. The chordal profiles at the selected time are then analyzed and used to characterize the flow pattern in terms of time evolution and characteristic shape and parameters. A detailed description of the methodology can be found in ref. [12].

The experimental facility (Fig. 2) consists of the feed water loop (tap water with conductivity of about 620 μS is used), the feed air loop and the test section. The liquid flow rate is measured with a ±0.5% r.v. accuracy value. The air flow rate is measured by means of different rotameters for the different ranges with a ±2% f.s.v. accuracy value. The test section consists of a 19.5 mm diameter and about 6 m long horizontal pipe. The WMS is located between two Plexiglas pipes having a length of 600 mm. Experiments have been performed at water temperature of about 20 °C. The flow quality ranges from 0 to 0.73 and the superficial velocity ranges from 0.14 to 31.94 m/s for air and from 0.019 to 2.62 m/s for water. The pressure ranges from atmospheric pressure to 3.7 bar depending on the experimental conditions. The typical observed flow patterns are stratified flow, intermittent flow (slug and plug) and non symmetric annular flow. The comparison between the observed flow patterns and the prediction by the Mandhane's map is reported in Fig.3; the flows are identified by superficial

velocities (J_g, J_l). Some runs have been performed in transition regimes on the ground of the visual observation and maps results.

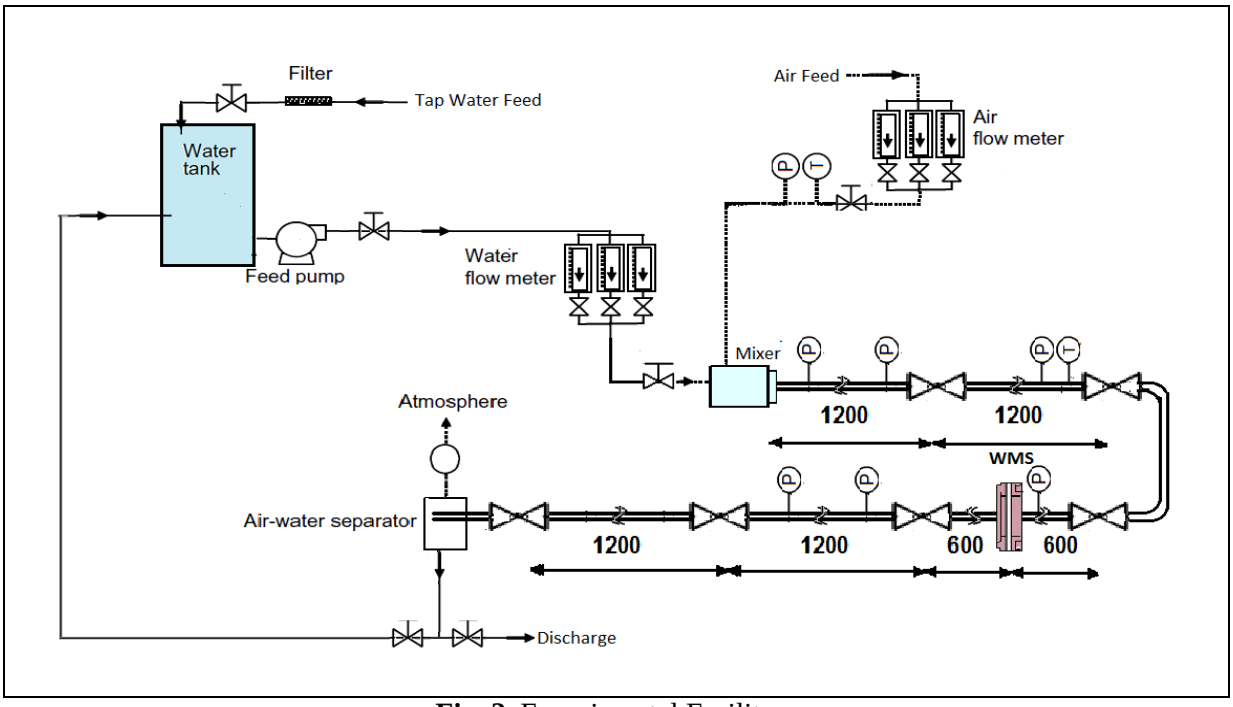

Fig. 2. Experimental Facility.

Legend: ST=Stratified, INT=Intermittent, AN=Annular, BUB=Bubble

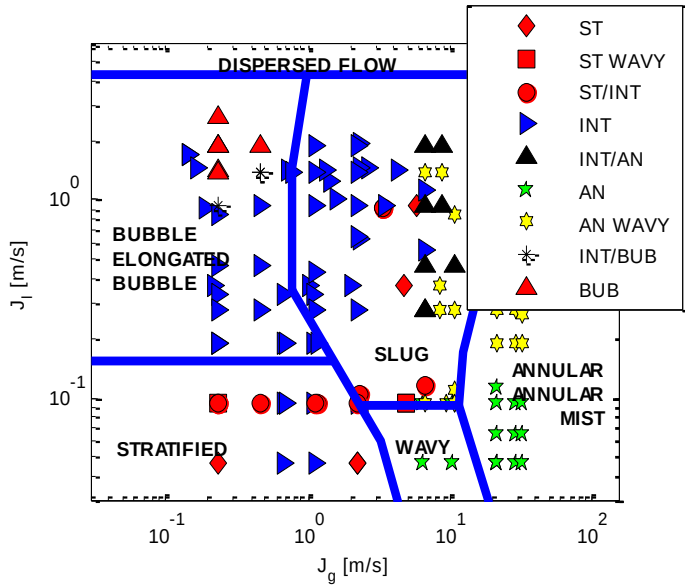

Fig. 3. Comparison between Mandhane's Map flow patterns prediction and visual observation.

To obtain a characteristic shape of the void fraction profile that can be related to the superficial flow velocities, the moving average profiles have been evaluated. In Fig. 4 the time evolution of the parameter *M(t)*, that is obtained using a moving average time τ of 0.4 s, is shown for different air and water superficial velocities.

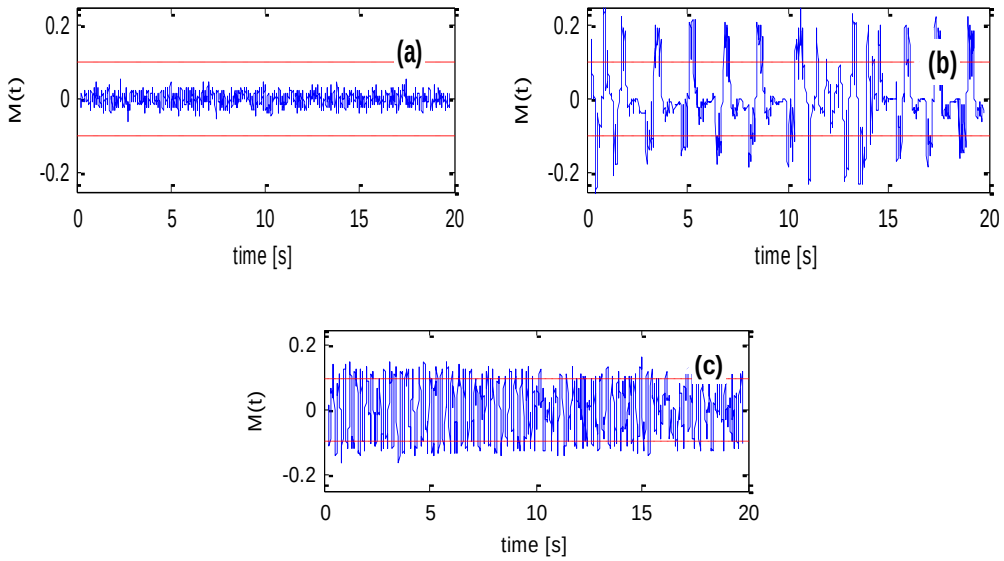

Fig. 4. *M(t)* time evolution at j=8. (a) J_g =0.23 m/s - J_l=1.86 m/s, (b) J_g =2.26 m/s - J_l =0.65 m/s, (c) J_g =8.73 m/s - J_l =1.86 m/s.

The optimum time interval, used for the moving average profiles, has been selected as the minimum averaging time that allows us to maximize the time period in which *M(t)* is zero. If the amplitude is lower than a threshold value the flow can be characterized by the mean profile and the correspondent standard deviation (Fig. 4 (a)), and it is classified as "non intermittent" or "non periodic profile" flow; while for higher amplitudes, (*M(t)* higher than 0.1 in absolute value) a number of profiles depending on the time history have to be analyzed. In this case the flow evolution can be divided in two categories, namely "quasi periodic profile" (Fig. 4 (b)) , and "non periodic profile with high noise" (Fig. 4 (c)): the profile is classified as "quasi periodic" if there is a time period in which the profile doesn't change significantly, while it is classified as "non periodic with high noise" if the absolute value of *M(t)* is higher than the threshold value and the local flow is characterized by a chaotic behavior. For the "high noise" profile, in which the value of the *M(t)* is continuously changing, the time evolution is characterized by the mean profile, that is evaluated adopting the observation time of 20 s, and by the relative standard deviation. For the "quasi periodic" profile at least two characteristic profiles with the related time are derived considering the time periods in which *M(t)* is near zero and the time periods in which the flow is evolving and *M(t)* is higher than zero. For classification purpose and considering the time interval that has been adopted to perform the moving average, the limit value has been considered of the order of 0.5 s: the profile is considered as "quasi periodic" if the profile doesn't change significantly for a period higher than 0.5 s. From the analysis of the parameter *M(t)* time evolution, the flow characteristic profiles are derived and qualified in terms of shape and flow parameters.

As an example, in Figs. 5 the characteristic void fraction chordal profile is shown for two different flows, that are characterized by low amplitude values of *M(t)*. In Fig. 5a the typical profile of an horizontal bubbly flow is shown, while in Fig.5b the flow can be classified as annular. Considering the flow of Fig. 5a, the parameters that have to be defined in order to classify it are: the height of the stratified region, the mean value of the void fraction in the bubbles region, the mean value of the void fraction and the related standard deviation in the stratified region, and finally the mean value of the void fraction in the upper part of the pipe, that is close to the wall. In order to characterize the annular flow the parameters like the liquid film thickness, the interface position, the average void fraction in the core region can be derived from the void fraction profile (Fig.5b).

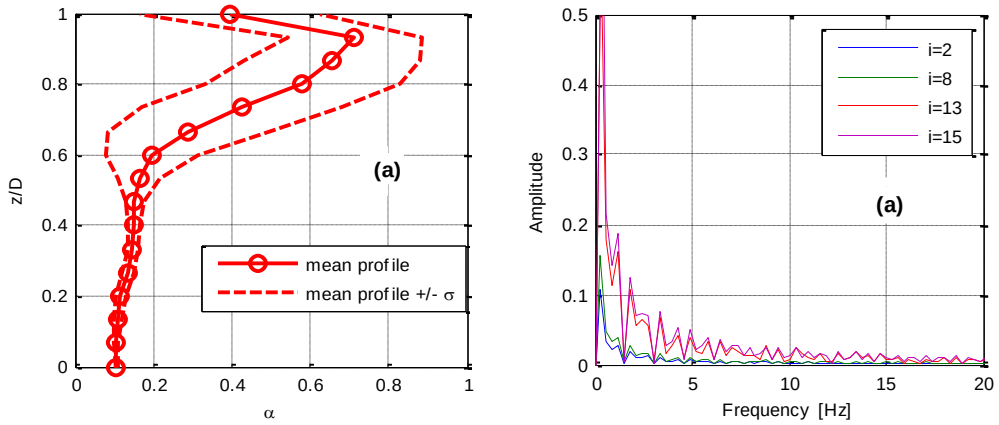

Fig. 5a. Characteristic void fraction chordal profile and Frequency spectrum for non-intermittent flow. (a) J_g =0.23 m/s – J_l =1.86 m/s, (b) J_g=29.3 m/s – J_l =0.05 m/s.

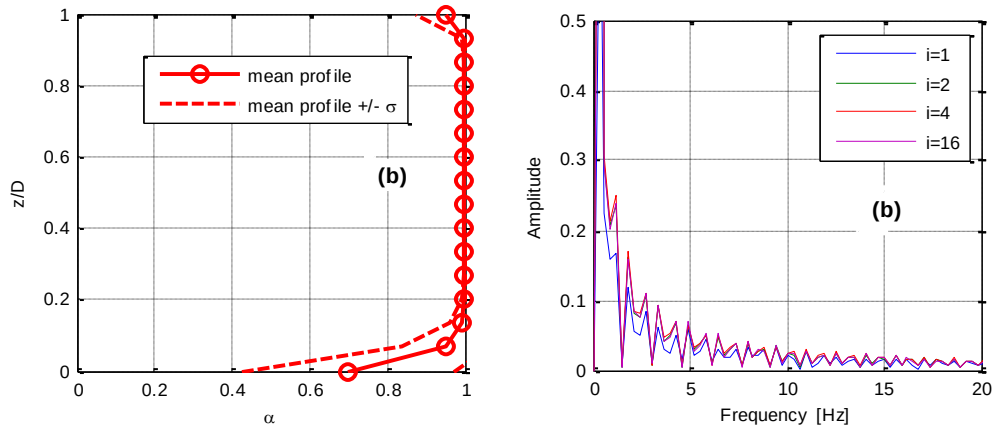

Fig. 5b. Characteristic void fraction chordal profile and Frequency spectrum for non-intermittent flow at j=8. (a) J_g=0.23 m/s – J_l =1.86 m/s, (b) J_g=29.3 m/s – J_l=0.05 m/s.

At higher water velocity the evolution from bubble flow to annular flow occurs; the air flow rate increase causes an increase of the void fraction and a reduction of the liquid film thickness both in the upper and lower region of the pipe. If the liquid velocity increases the flow tends to homogenize with a void fraction at the channel bottom higher than zero while the maximum void fraction value decreases. By increasing the air velocity the mean chordal void fraction increases and the profile flattens evolving in annular flow. The transition to the annular flow seems to coincide with a shift of the void fraction maximum value towards the centre of the pipe. The pictures in Fig. 6 show that the flow is symmetric with respect to the vertical pipe axis and the profile of the void fraction is strongly affected by the gravity effect. The flow can be classified as plug flow and it is characterized by a deterministic time evolution of the void fraction, with the lower part of the pipe (up to *j*=6) always covered by the liquid phase, while in the upper part of the pipe, large bubble of gas (plugs) are spaced out by slugs of liquid. The void distribution for the flows classified as bubbly is quite different depending on the liquid velocity. The comparison of the chordal profiles at different superficial velocities combinations of water and air, is pointed out in Fig. 7 showing the effect of the superficial velocities on the vertical profiles. The developed methodology for the analysis of the Wire Mesh Sensor signals allows the identification of the flow pattern and the flow characterization in terms of void fraction profiles and characteristic times. From the analysis of the time evolution of the local void fraction and of the parameter *M(t)* it is possible to characterize the flow in terms of the void fraction profile shape and other parameters like phases distribution, liquid level, mean void fraction in the

different pipe regions, characteristic frequencies. The evolution of the void fraction profiles, related to the superficial velocity of the two-phases (J_g and J_l), and the flow evolution in time and space show that such methodology is useful to identify and characterize the two-phase flow patterns. All the test results are reported in refs. [7] and [12].

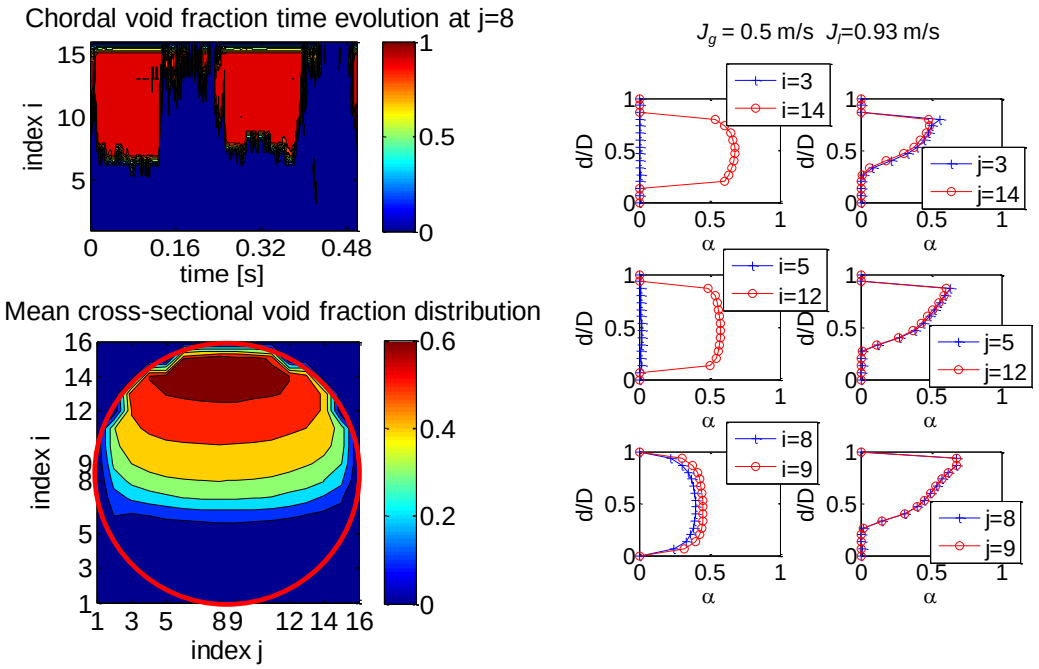

Fig. 6. Plug flow example: J_l=0.93 m/s and J_g=0.5 m/s.

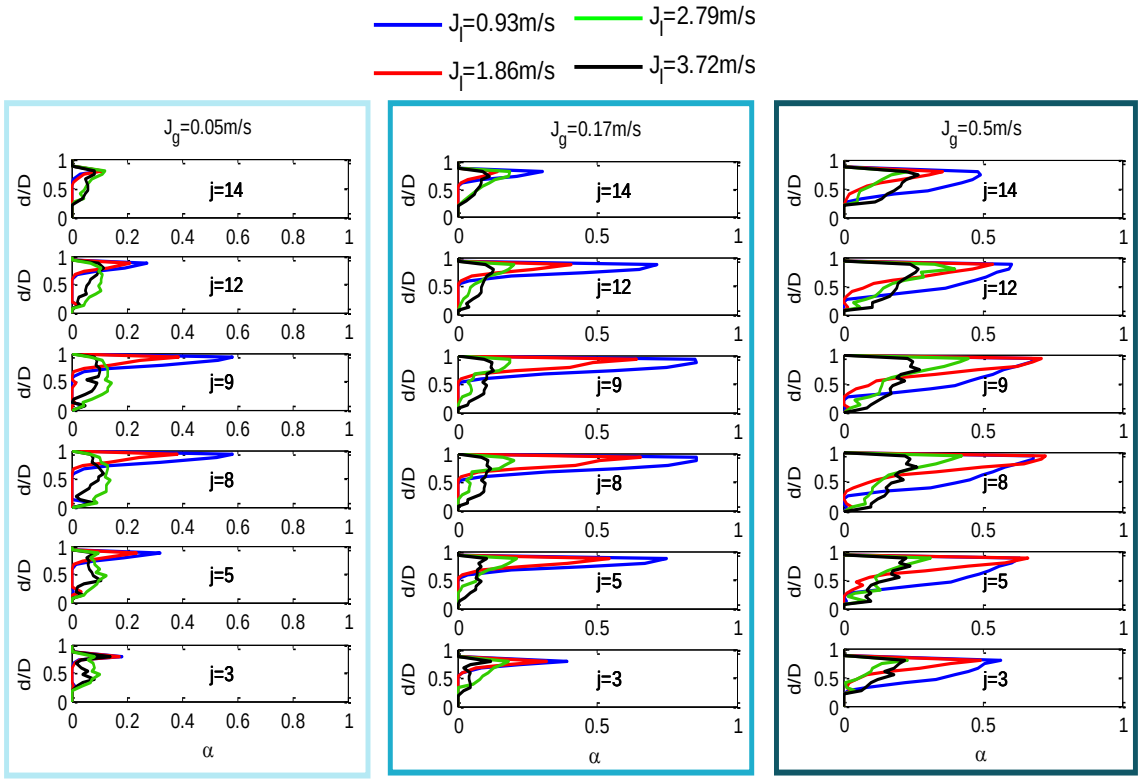

Fig. 7. Velocities dependence: Vertical Profiles.

3. Two-Phase Flow Measurement for Nuclear applications in Simulation Facilities

3.1 Spool Piece: Turbine-Drag Disk-Impedance Probe

The SP consisting of a turbine flow meter (TFM), a drag disk (DD) has been one of the most analyzed instruments combination during the first experimental tests for nuclear reactors [13].

In the present study a SP made up of three instruments, turbine, drag-disk and a concave electrodes impedance probe, has been analyzed. The test section where the SP is installed is part of the facility shown in Fig. 8: the main components of the facility and the instruments of the SP (1- Impedance probe, 2- Turbine and 3- Drag Disk in the picture below it), are schematically reported in Fig. 8.

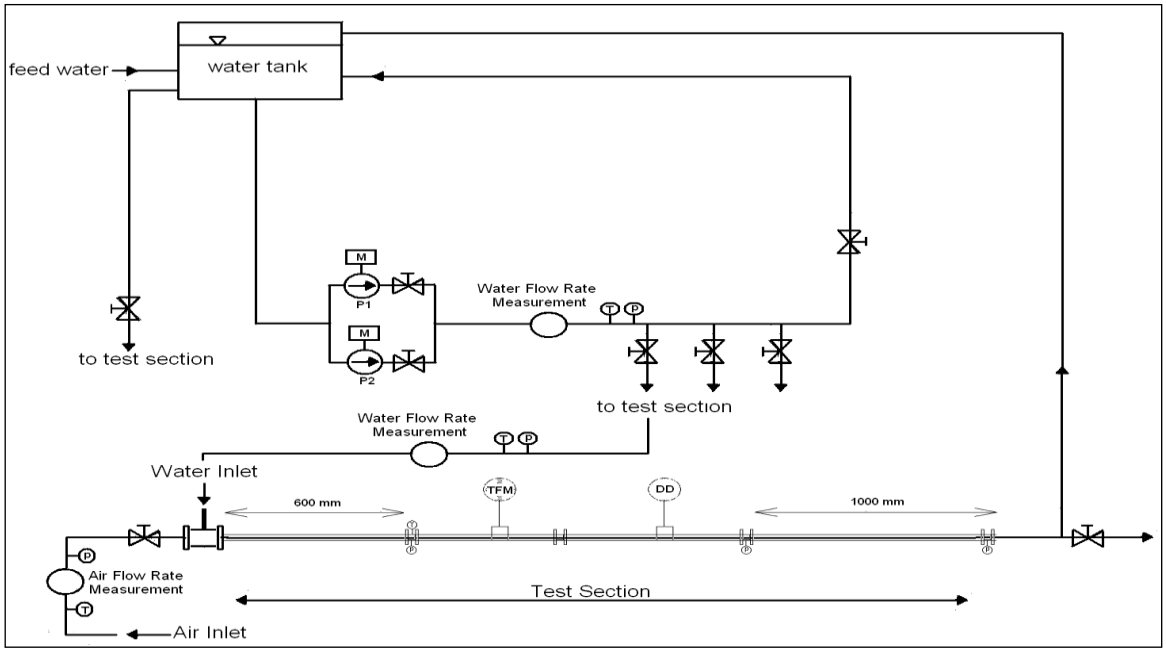

Fig. 8. Experimental facility and test section picture.

The turbine flow meter and the drag disk have been calibrated under single-phase flow, and then the response of the instruments of the SP have been analyzed in two-phase flow between 0.055 and 0.3 kg/s and 0.005 to 0.013 kg/s for water and air respectively.

As regards the turbine, an example of the dependence of the signal on the mass flow rate of the phases is shown in Fig. 9.

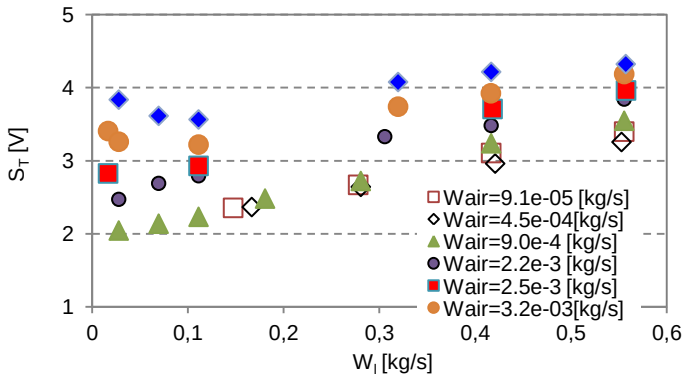

Fig. 9. Turbine signal S_T vs. water mass flow rate at different air flow rate.

The non linear behavior is evident for higher air mass flow rate; for lower values of the air flow rate the signal is monotonically increasing. The turbine signal depends on the pressure as the fluid is compressible but the test runs have been carried out at constant pressure.

For the drag disk the signal dependence on the mass flow rate of the two phases has been analyzed as shown in Fig. 10.

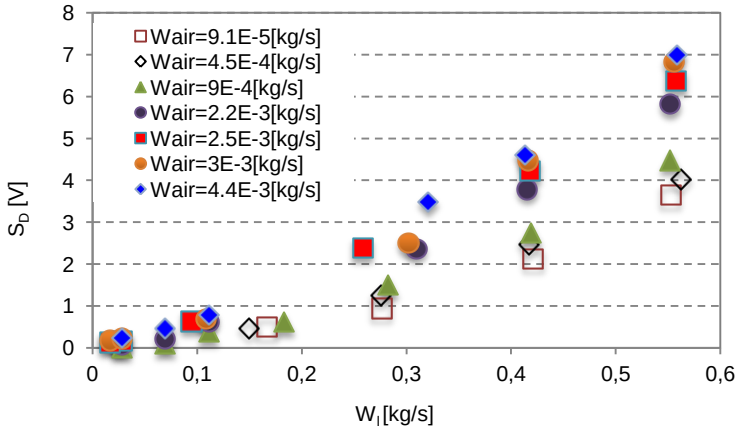

Fig. 10. Drag disk signal S_D vs. water flow rate at different air mass flow rate

The quadratic relationship between mass flow rate and sensor signal is observed at all the experimented flow rates. The signal of the drag disk tends to increase with both the air flow rate and water flow rate.

The impedance probe (IP) installed in the SP (fig.11), consists of two concave externally mounted electrodes having a length of 166 mm and a width of 18 mm. The two electrodes are installed at 180° along the axial length of the pipe.

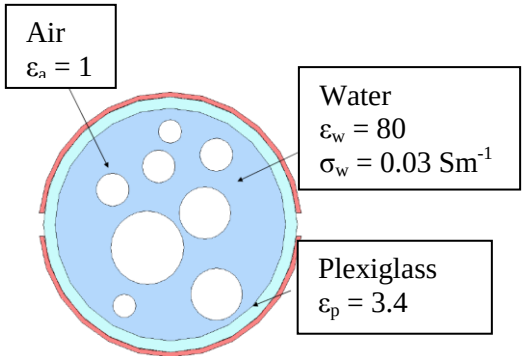

Fig. 11. Scheme of the IP cross-section and electrical properties of the materials.

The signals are acquired for 30 s, using a sample frequency of 1 kHz. At each run the volumetric void fraction is measured by means of two Quick Closing Valves (QCV) after the signal acquisition. The volumetric void fraction is measured 5-10 times at the same flow condition in order to have a sufficient statistics. The tests provided data points for $0.2<\alpha<0.9$. The observed flow patterns have been related with the measured void fractions: bubbly and slug flows are confined to low-range flow quality with void fractions ranging between 0.2-0.45 and 0.45-0.7 respectively, while annular flow has been observed for void fraction ranging between 0.7 and 0.9. The impedance probe analysis has been performed comparing the signal with the experimental volumetric void fraction measured by means of the QCV, dividing the data into groups depending on the flow pattern (Figs. 12 and 13).

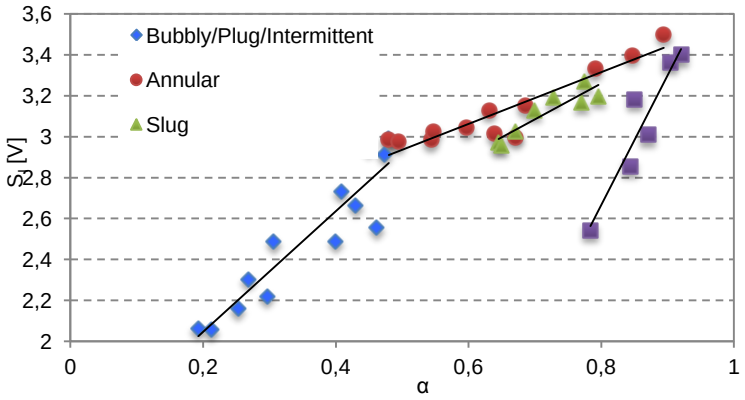

Fig.12. Impedance probe signal vs. void fraction.

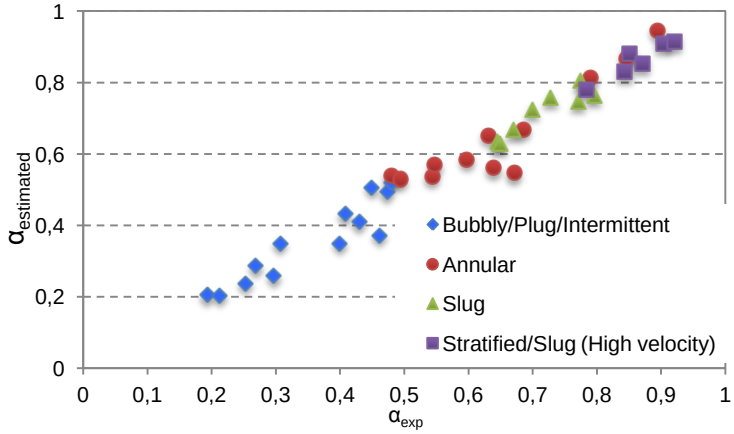

Fig. 13. Impedance probe experimental void fraction vs. estimated void fraction.

The Aya's model [14] has been used to calculate the mass flow rate of the two phases, adopting in this case a turbine coefficient equals to the water single-phase flow coefficient, and evaluating the void fraction by means of the developed model of the impedance sensor. The parametric analysis, performed by the Aya's model, has shown that, the knowledge of the flow pattern, and then of the void fraction, is required to evaluate the two-phase flow parameters. So the SP has been completed with the third instrument able to measure the void fraction of the flow (an impedance sensor), whose signal has been analyzed as a function of the flow parameters and compared with the experimental volumetric void fraction measured by means of the QCV. The analysis shows that a linear relationship between void fraction and impedance sensor can be used, but the knowledge of the flow pattern is needed for a proper signal interpretation. The experimental data, corresponding to different flow patterns from bubbly to annular flow, have been used to get an operating map of the SP, able to evaluate the mass flow rates of the phases in the mixture, with the relative errors, and to predict the flow pattern. The measurement of the void fraction allows the use of the Aya's model in all the experimented range, obtaining the mass flow rate of the phases with an accuracy of 15% in the 75% of the cases.

Fig. 14 shows that most of the points calculated with the model of Aya are in the range of 15% of error, which means that the data has been obtained correctly. It can be concluded that the results of a SP, consisting of a turbine flow meter, a drag disk and an impedance concave probe, under annular and stratified annular air-water two-phase flow, have allowed the characterization of the flow in terms of flow pattern and mass flow rates of the phases, with an accuracy of 15%, in the experimented range. Further details can be found in ref. [15].

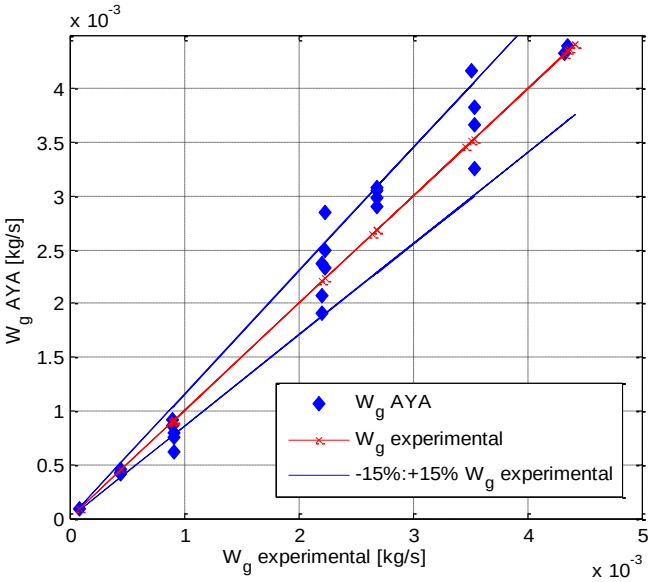

Fig. 14. Air mass flow rate (W_g) experimental vs. W_g predicted by Aya's model.

3.2 Spool Piece: Venturi Flow Meter (VFM) and WMS

In the second analyzed SP, the Wire Mesh Sensor (WMS), presented in section 3.1 and a classical Venturi Flow Meter (VFM) have been installed in horizontal configuration and analyzed under air-water two-phase flow. Compared with single-phase flow, the two-phase flow VFM pressure drops increase due to the interaction between the gas and the liquid phase; for this reason the value of the effective two-phase mass flow rate must be estimated using available correlations derived from experimental data or semi-empirical models.

The test section described previously has been modified with the insertion of the second instrument (Fig. 15). It consists of a 19.5 mm diameter and 7 m long pipe. The SP is installed at L/D = 192 from the entrance; the WMS is installed between two Plexiglas pipes having a length of 600 mm, while the VFM is installed between two Plexiglas pipes having a length of 500 mm and 490 mm upstream and downstream respectively. The experimental test section is equipped with two quick closing valves (QCV) that allow the measurement of the volumetric void fraction in a length of 1300 mm. The signals have been acquired using a frequency f = 1250 Hz for all the instruments for a total acquisition time of 20 s. Instruments characterization in single-phase flow of air and water has been performed. The flow quality ranges from 0 to 0.73 and the superficial velocity from 0.14 to 32 m/s for air and from 0.019 to 2.62 m/s for water.

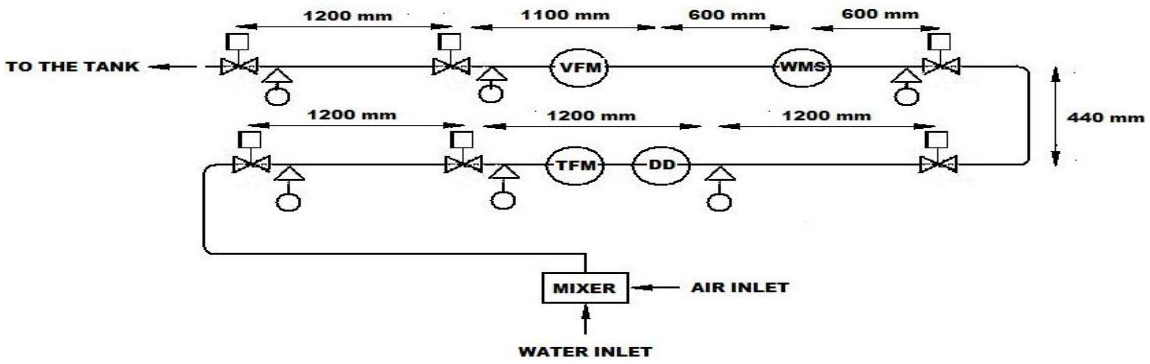

Fig. 15. Test section schematic.

According to Baker's Map [16] the typical observed flow patterns were stratified flow, intermittent flow (slug and plug) and annular flow. The WMS output signal *V(i,j,k)* is analyzed in order to obtain the mean cross sectional value of the void fraction, that is used to model the response of the VFM. The local instantaneous void fraction (eq.1) has been obtained with an acquisition frequency f_{acq} equal to 1250 Hz for a total observation time T_T equal to 20 s, so that the value of k ranges from 1 to k_T, where k_T is the total number of measured frames, equals to $f_{acq} \cdot T_T$.

The averaged time cross-sectional void fraction is obtained by averaging over the observation time and over the measuring section (A_p is the pipe cross section):

$$\langle \alpha \rangle = \frac{1}{k_T} \sum_{k=1}^{k_T} \frac{1}{A_p} \sum_{i=1}^{16} \sum_{j=1}^{16} \alpha(i, j, k) \tag{3}$$

The WMS experimental void fraction has been then compared with different literature correlations (Lockhart-Martinelli [17], Baroczy [18], Chisholm [19] and Wallis [20]): the Lockhart-Martinelli and Wallis correlations give a good estimation of the experimental data at flow qualities higher than 10^{-2}. In order to estimate the momentum density, the void fraction value must to be known; then the output of the WMS becomes an input for the VFM signal interpretation. The two-phase flow discharge coefficient is then evaluated, based on the experimental data [7].

The SP model consists of a set of equations that, based on the measurement of the VFM pressure drop, and on the measurement of the void fraction in the WMS, together with the measurement of pressure and temperature of the fluid, allows the estimation of the mass flow rate of the phases in the test section:

$$\begin{cases} x = f_1(\alpha) \\ J_l = f_2(\alpha, \Delta p_{VFM}, p) \\ J_g = f_3(\alpha, \Delta p_{VFM}, p) \end{cases} \tag{4}$$

An iterative approach is adopted for the estimation of the two mass flow rate of the phases. The model input are the void fraction, the pressure drop in the VFM, and the properties of air and water that are evaluated at the working pressure and temperature. An initial guess value for the flow quality is introduced. Using a *x-α* correlation the void fraction is calculated and the flow quality value is iterated till the error between the void fraction calculated and the void fraction measured by the WMS is lower than a threshold value. When the required accuracy is reached, the two-phase flow Reynolds number and the discharge coefficient are calculated in a new iterative loop, where for the first iteration the discharge coefficient for the liquid is assumed. When the convergence is got ($W_{TP,i} - W_{TP,i-1} < 10^{-4}$) the mass flow rate are calculated for the two phases.

For the *x-α* correlation to be used in the calculation, the Lockhart-Martinelli correlation has been modified, based on present experimental data.

$$\begin{cases} \alpha = \left[1 + 0.2 \cdot \left(\frac{1-x}{x} \right)^{0.6} \cdot \left(\frac{\rho_g}{\rho_l} \right)^{0.36} \cdot \left(\frac{\mu_l}{\mu_g} \right)^{0.07} \right]^{-1} & x < 1 \cdot 10^{-3} \\ \alpha = \left[1 + 0.28 \cdot \left(\frac{1-x}{x} \right)^{0.6} \cdot \left(\frac{\rho_g}{\rho_l} \right)^{0.36} \cdot \left(\frac{\mu_l}{\mu_g} \right)^{0.07} \right]^{-1} & 10^{-3} \le x \le 6 \cdot 10^{-2} \\ \alpha = \left[1 + 0.45 \cdot \left(\frac{1-x}{x} \right)^{0.6} \cdot \left(\frac{\rho_g}{\rho_l} \right)^{0.36} \cdot \left(\frac{\mu_l}{\mu_g} \right)^{0.07} \right]^{-1} & x > 6 \cdot 10^{-2} \end{cases} \tag{5}$$

The comparison between the original correlation, the modified correlation and the void fraction value obtained from the WMS signal analysis is shown in Fig. 16.

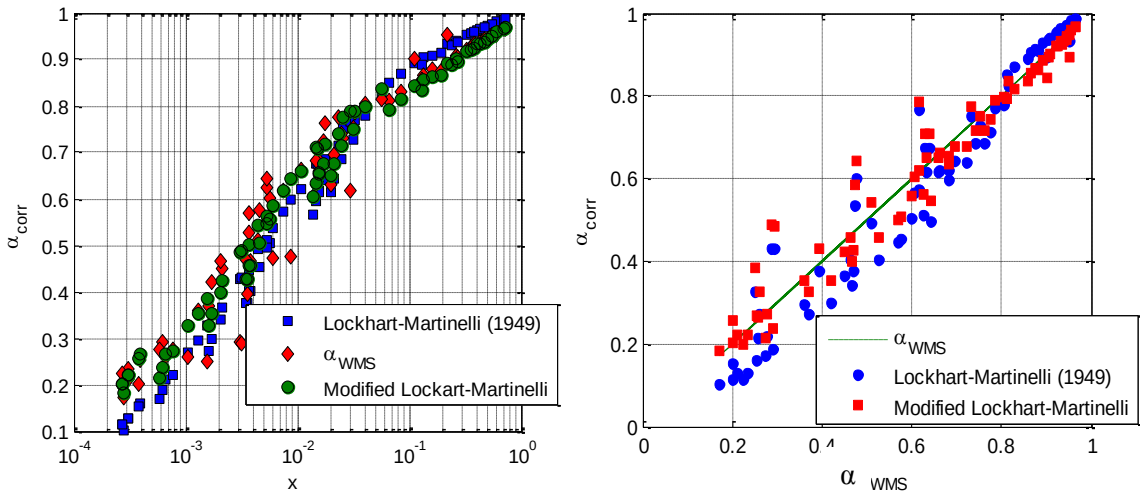

Fig. 16. Comparison between WMS void fraction and correlations.

The developed SP Model has been applied to the experimental data in order to derive the mass flow rate of the phases. The flow quality is estimated with an error lower than 10% for the 72% of the runs. The estimated mass flow rates are shown in Fig. 17. The mass flow rate has been estimated with an error lower than 10% in the 73.3% of the cases and the estimation error is considerably lower for the flow characterized by higher values of quality and void fraction. In this range, with reference to facility SPES3 test conditions, the error in the mass flow rate estimation is always lower than 10% and 20% for water and air respectively.

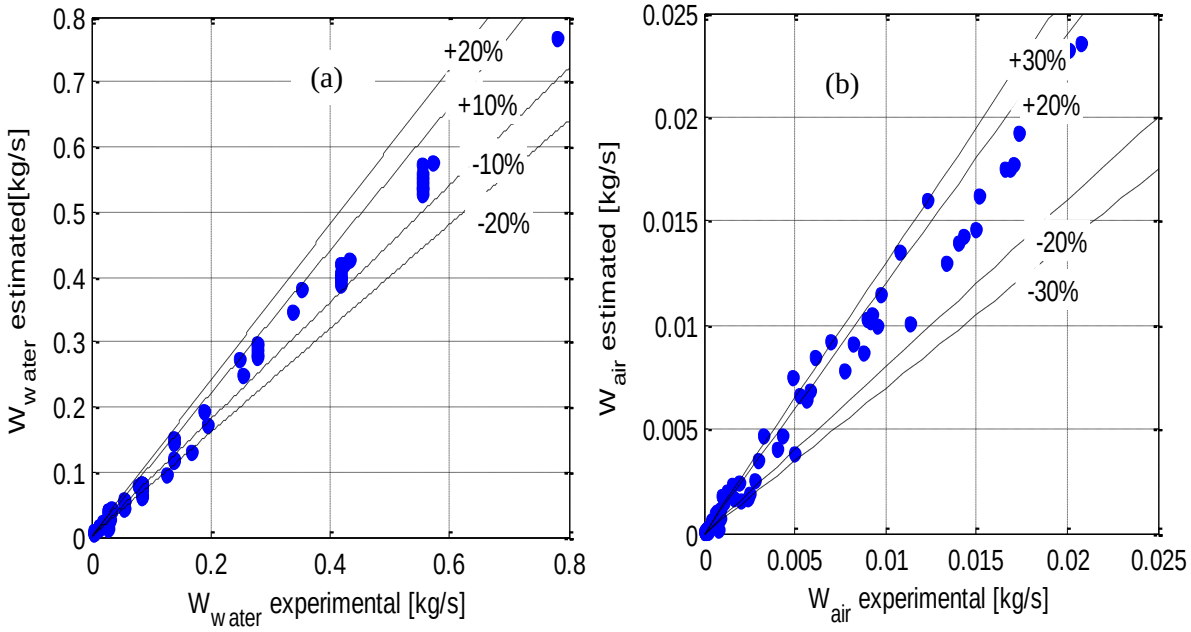

Fig. 17. Experimental mass flow rate vs. SP mass flow rate for water phase (a) and air phase (b).

3.3 Electrical Capacitance Probe (ECP)

The electrical sensor designed at the SIET laboratories [21, 22, 23], for the measurement of the void fraction in the SPES-3 break lines, has been developed in order to be inserted in a SP for the measurement of the mass flow rate of the phases. The range of interest of the flow parameters in the SPES3 facility, in steady state and transient conditions, has been investigated by means of the RELAP-5 code [24]: the simulations show that in a relative long period of the transients, the two-phase flow corresponds to an annular flow pattern, characterized by very high void fraction and high flow velocity, so the selected instruments of the Spool Piece must be sensitive to the flow in such conditions. The sensor (ECP) consists of 10 electrodes: 9 external and one internal (Fig. 18 a). The internal and the external diameters of the Plexiglas pipe, where the probe is mounted, are 80 mm and 90 mm respectively. The external electrodes (steel stripes of 400 mm length and 5 mm width) are spaced with 22.5° angle only in half of the pipe circumference, as the symmetry of the vertical flow has been verified. The angle corresponds to an external chord of 17.56 mm and an internal chord of 15.6 mm. Details can be found in ref. [21]. The main purpose of the sensor is the evaluation of the effect of the angular electrode distance on the output signal.

The experimental test section (Fig. 18 b) consists of the feed water and the feed air loops equipped with instruments to measure the single-phase flow parameters (flow meter, temperature and pressure). Details can be found in ref. [23]. The first ECP qualification step is the characterization of the sensor for single-phase conditions [23].

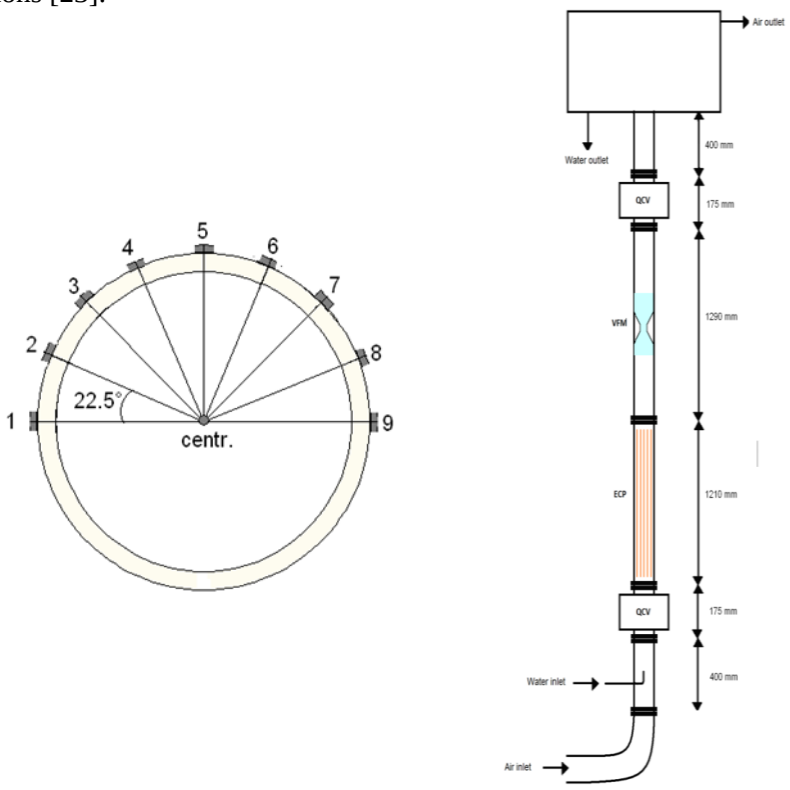

Fig. 18. Schematic of the ECP (a) and of the test section (b).

In order to evaluate the response of the sensor at high void fractions, corresponding to annular flow, preliminary tests at atmospheric pressure have been carried out with a mixture of air and demineralized water introduced in the test section. The mass flow rate ranges from 0.094 to 0.15 kg/s for air and from 0.002 to 0.021 kg/s for water, corresponding to a void fraction higher than 95%. In

order to take into account the single-phase signal variations, the two-phase flow measured values are normalized as follows:

$$V_{ij}^{*} = \frac{RMS_{TP-ij} - RMS_{l-ij}}{RMS_{g-ij} - RMS_{l-ij}} \tag{5}$$

where the subscript *ij* identifies the measuring electrodes combination. As an example of the preliminary results, the average signals measured between electrodes at 22.5°, 45°, 90° and 180° are presented in Fig. 19 as a function of the volumetric void fraction measured by the QCV technique. V_{ij}* , evaluated by means of the eq. (5), increases with θ at constant void fraction, and approaches the air value at higher angular distance.

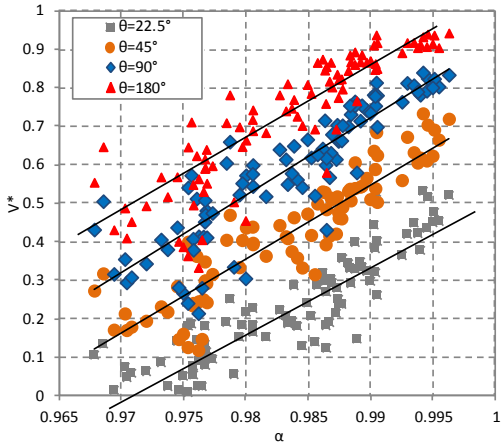

Fig. 19. Mean signal in the external electrodes as a function of the volumetric void fraction α.

Due to the symmetry of the flow, the annular flow regime in a vertical channel can be analyzed as a liquid film region and a core region with entrained droplets. The liquid film is characterized in terms of film thickness, frequency and amplitudes of the waves at the liquid-gas interface, while the core region is characterized in terms of the mean void fraction value.

Adopting the Ishii correlation [24] for the fraction of the liquid flux flowing as droplets entrained in the vapor core, the liquid film thickness is shown in Fig. 20.

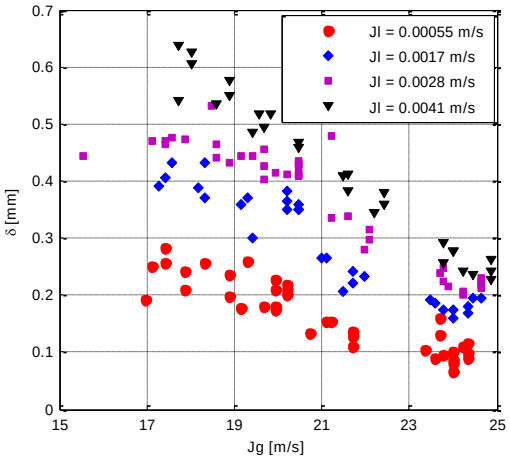

Fig. 20. Mean film thickness as a function of the experimental water and air superficial velocities.

In the second experimental campaign, when downstream of the ECP a VFM has been installed between two straight pipes of 1290 mm upstream and downstream (Fig.20 b), the air superficial velocity range is between 14 and 18 m/s while the water superficial velocity ranges from 0.0008 to 0.005 m/s; the flow pattern is annular and the corresponding void fraction is higher than 0.97, while the flow quality ranges from 0.78 to 0.96. The ECP response has been studied by means of a FEM analysis, able to evaluate the sensitivity of the sensor to the void fraction variation in the measurement volume. The FEM analysis allows the evaluation of the capacitance associated with the different measuring electrodes, for the different phases distributions, by means of the electrical field resolution in the control volume. Three different phases distribution are simulated: homogeneous, ideal annular flow, annular flow with entrainment (thin and smooth liquid film at the pipe wall and a homogeneous mixture in the core region). In the last case the void fraction value depends on the liquid film thickness and on the dielectric constant of the mixture in the core region. The numerical analysis highlights that the electrodes response strongly depends on the phases distribution.

The signal obtained under two-phase flow conditions is normalized as reported in eq. 5. As an example in Fig. 21 the comparison between experimental and numerical data is shown for the external electrodes characterized by a measuring distance of 22.5° and 180°, showing the dependence on the void fraction and on the liquid film thickness (C^* is the normalized electrical capacitance). The comparison shows a qualitative good agreement of the experimental data with the numerical predictions and that the electrode, characterized by a measuring distance of 180°, shows a very low data dispersion and a linear dependence on the mean cross sectional void fraction that highlights a similar behavior under homogeneous and annular flow.

The performed analysis allows us to conclude that the signal related to the electrodes at 180° can be used to directly estimate the average cross sectional void fraction, due to the low sensitivity to the phases distribution, while the measurement at 22.5° can be useful for the liquid film thickness and the core phases distribution.

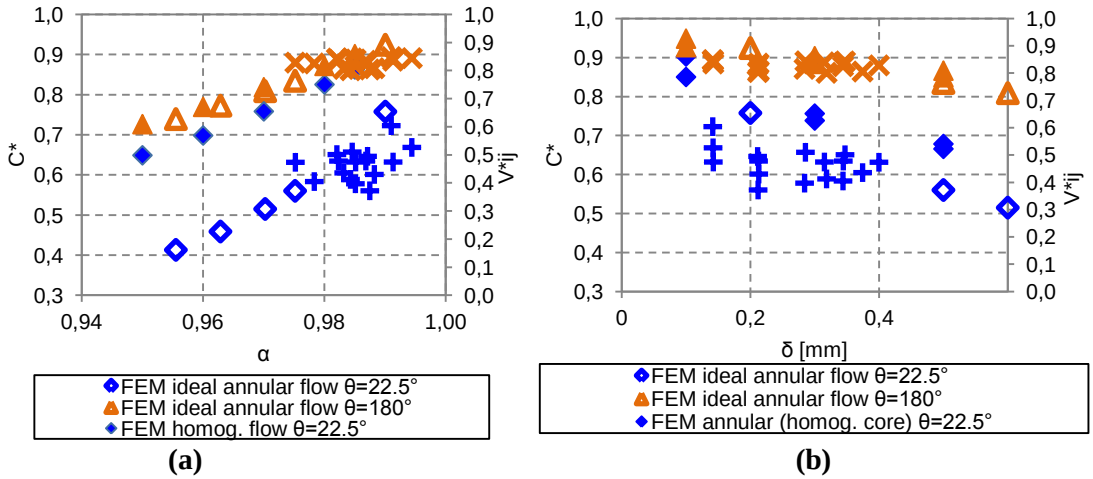

Fig. 21. Comparison between experimental and numerical ECP external electrodes results at 22.5° and 180°. Void fraction dependence (a) and film thickness dependence (b).

In Fig. 22 the comparison between numerical and experimental results for the central electrode is reported. Also in this case the comparison shows a good agreement between the experimental measurement and the simulations corresponding to the ideal annular flow. Although the sensitivity of the Electrical Capacitance Probe (ECP) in single-phase flow is low, two-phase flow void fraction variations lower than 1% has been detected.

The presence of the central electrode allows the evaluation of the average cross-section void fraction also in annular flow, where the liquid film is the principal cause of the sensor low sensitivity. The signal measured in the central electrode is linear with the void fraction for values higher than 98% and it is quite sensitive to the flow pattern (flow patterns, from rather regular to more disturbed annular flow, have been clearly characterized). The variation of the signal measured in the external electrodes has been related to the average liquid film thickness that is evaluated by means of the Ishii's model [24]. The sensitivity of the sensor must be increased, in order to make the instrument suitable to be used for void fraction measurement with a good accuracy. The FEM numerical model, compared with the experimental data, shows a good agreement and the possibility to use it to identify the possible sensor modifications finalized to increase the sensitivity under annular flow conditions.

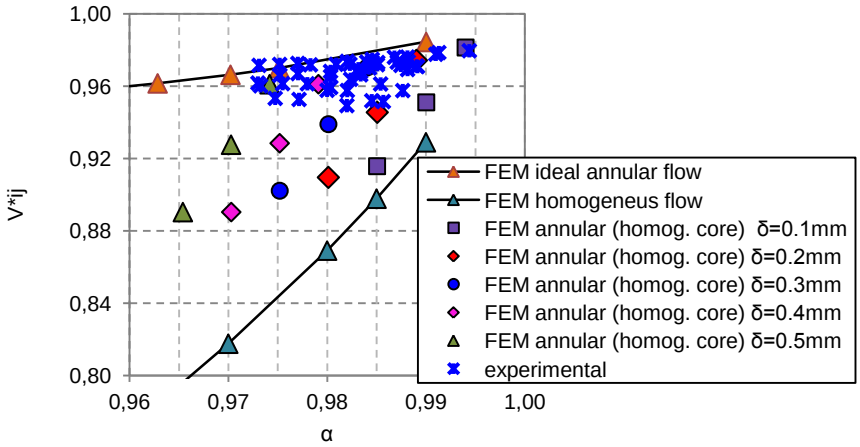

Fig. 22. Comparison between experimental and numerical ECP central electrode results as a function of the void fraction.

3.4 Venturi flow meter in vertical annular flow

Two Spool Pieces have been previously presented for horizontal flow, consisting of a Turbine Flow Meter and a Drag Disk and of a Venturi Flow Meter and a Wire Mesh Sensor [26]: if the void fraction, and then the flow pattern, can be correctly identified, the two instruments can be used to estimate the mass flow rate of the two phases with a good accuracy. A similar approach has been applied in a vertical test section, where a new Venturi Flow Meter has been coupled with the Electrical Capacitance Probe (Fig. 18 a). The VFM (80 mm maximum diameter, 340 mm total length) has been home designed and has been constructed in Plexiglas in order to allow the visualization of the flow (Fig. 23).

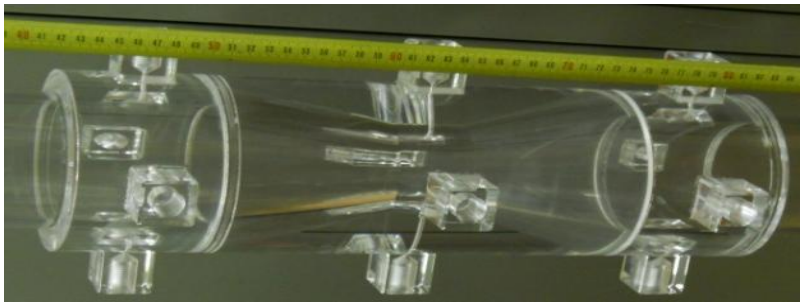

Fig. 23. Venturi Flow Meter picture.

The air superficial velocity range is between 14 and 18 m/s while the water superficial velocity range is between 0.0008 and 0.005 m/s, to have an annular flow pattern, and the corresponding void fraction is higher than 0.97, while the flow quality ranges from 0.78 to 0.96. The Venturi has been designed to operate in both fluid direction (symmetrical flow meter), with the angle of the convergent section equal to the divergent section angle (θ=21°), in order to be able to work in reverse flow conditions. Compared with the Herschel model the present VFM is characterized by a higher divergent angle (usually set to 15°), with higher irreversible pressure drops, due to the flow separation. In single-phase flow the discharge coefficient value takes into account the phenomena of the wall flow detachment at the inlet of the divergent section.

According to the well known approach, the frictional pressure gradient of a two-phase mixture flowing in a pipe can be correlated to the single-phase pressure drop by means of the two-phase flow multiplier [27], that is expressed by empirical or semi-empirical correlations (Chisholm [28], Murdock [29]). The mixture void fraction is measured by means of the QCV technique. The acquisition time is equal to 30 s with an acquisition frequency of 1250 Hz. The pressure drop values across the Venturi, reported in ref. [7], show the dependence on the superficial velocities of the two phases and the small effect due to the liquid flow rate. The flow field is characterized and complicated by the continuous deposition and entrainment of liquid droplets along the Venturi length and by the presence of waves on the liquid film surface.

On the ground of the previous considerations, the pressure drop in the VFM can be expressed as a function of the single-phase pressure drop with a correction factor (a two-phase flow multiplier) that can take into account the presence and the effect of the liquid phase at different flow qualities. The two-phase flow multiplier can been written as:

$$\phi^2_{g,\mathrm{mod}} = 7.8 \cdot \chi + 1 \qquad (6)$$

where the two constants have been obtained as best-fit of the present experimental data.
The two-phase flow multiplier values, evaluated by the correlation (6), are compared with the correlations of Murdock, Chisholm and the present test data (Fig. 24): the classical correlations under predict the two-phase multiplier ϕ^2_g.

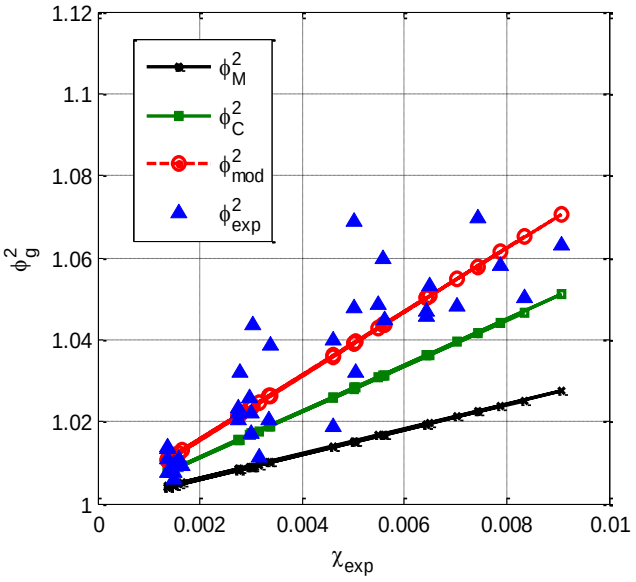

Fig. 24. Two-phase flow multiplier: comparison between experimental data and correlations.

In Fig. 25 the pressure drops evaluated with the new correlation are compared with the experimental values, showing a good agreement and a calculation accuracy better than 5%.

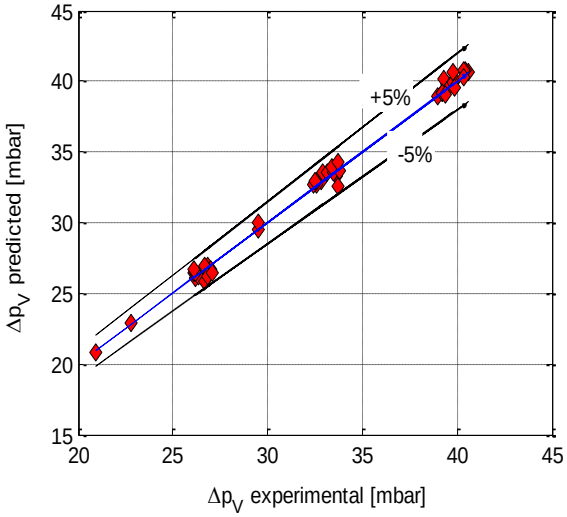

Fig. 25. VFM pressures drops: comparison between experimental data and predicted values (eq. 6).

The irreversible pressure losses, measured between the Venturi inlet and outlet sections have been correlated with the flow parameters. The analysis of this component allows us to understand better the effect of the dispersed phase in the two- phase pressure drops. Fig. 26 shows the dependence of the irreversible pressure loss on the superficial velocities of the phases. While, due to the liquid phase presence, the inlet-throat pressure drop increases of about 10%, if compared to the single-phase flow, the irreversible pressure loss increases from about 20% to 100% depending on the liquid flow rate.

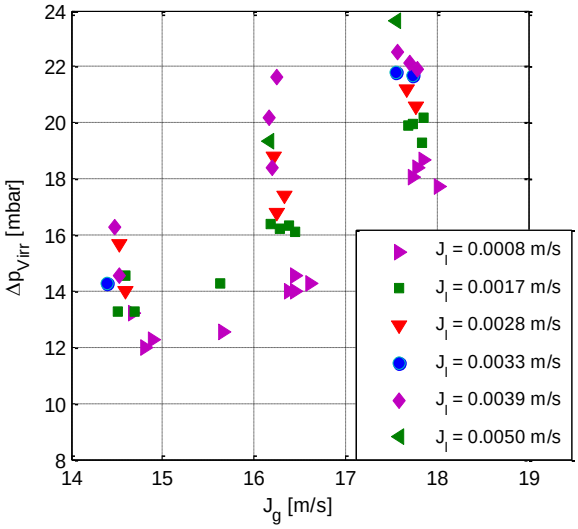

Fig. 26. VFM irreversible pressure loss as a function of the superficial velocities of air and water.

The previous analysis allows the derivation of a correlation able to describe the irreversible pressure loss change as a function of the flow rate of the two phases. The proposed correlation, developed for the present tested conditions, expresses the irreversible pressure loss as a function of the gas superficial velocity and of the ratio between the liquid and the gas superficial velocities, highlighting the effect of the dispersed phase:

$$\Delta p_{irr} = k_1 \cdot \left(\rho_g J_g^{k_2}\right) \cdot \left(J_l / J_g\right)^{k_3} + k_4 \qquad (7)$$

The following constants have been obtained from the best fit of the present experimental data: k_1 = 0.2096, k_2 = 2, k_3 = 0.13, k_4= -2.9786.
The comparison between the predicted irreversible pressure loss and the test data is shown in Fig.27: the proposed correlation allows the estimation of the VFM irreversible pressure loss, in annular flow, at high void fraction, with an accuracy of 5%.

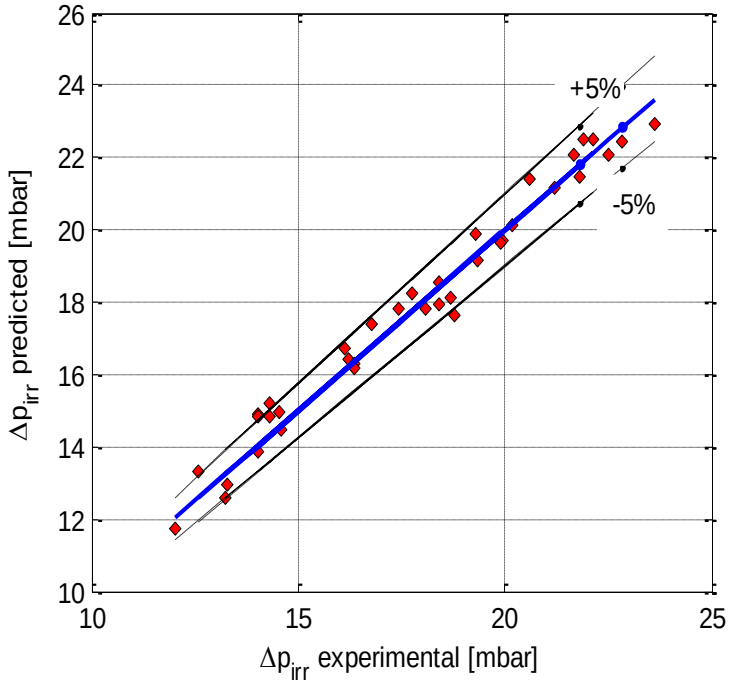

Fig. 27. Comparison between predicted (eq.7) and experimental VFM irreversible pressure losses.

In single-phase flow the VFM allows the estimation of the mass flow rate from the pressure drop across the pipe restriction, but in presence of two phases the direct correlation between pressure drops and mass flow rate is not possible, so additional information and a model able to interpret the signals are required [26,30]. In limited application ranges, if the flow pattern doesn't change, as in the present experimental conditions, it is possible to derive the essential information from the signals of a VFM. The closure equation of the model in this case is based on the measurement of the irreversible pressure losses and on the proposed correlation (7).

By means of an iterative approach the flow quality and the mass flow rate of the two phases have been evaluated: in the first iteration the air flow rate is guessed by considering a single-phase flow in the VFM, while starting from the second iteration this value is corrected using the estimated value of the flow quality, by using the correlation (6); an initial guess value of this parameter is used to evaluate the VFM pressure drops, and the iterative loop goes on until the estimated pressure drop reaches the experimental value. Then the mass flow rates of the two phases are estimated by using the flow quality value and the VFM pressure losses correlation (7). The reference signals have been obtained as the mean values of the 30 s acquisition time.

In Fig. 28 the estimated mass flow rates of air and water are compared with the values measured by the rotameters: the air mass flow rate is estimated with an accuracy of 2%, while a lower accuracy characterizes the liquid flow rate prediction (the relative error is lower than 30% for all conditions). All the details are given in ref. [7].

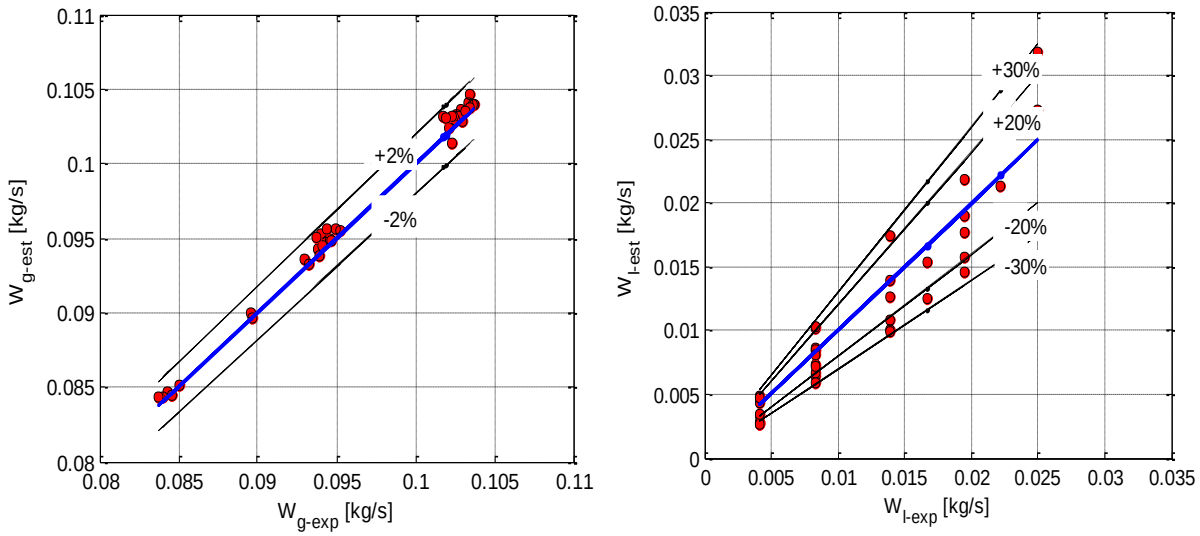

Fig. 28. Comparison between VFM experimental and estimated mass flow rates.

4. Conclusions

The performance of different measurements instruments has been evaluated in two-phase flow applications (like the simulation of nuclear plants accidents) and interpretative models for each one, as well as, experimental correlations for the quality - void fraction and for the pressure drops, have been developed and tested.

The developed WMS signal analysis allows to evaluate the relation between the evolution of the void fraction profiles and the superficial velocity of the two-phases (Jg and Jl). The flow evolution in time and space has been analyzed and discussed, showing that such methodology is useful to identify and characterize, in terms of void fraction characteristic profiles, characteristic frequencies and interface evolution, the two-phase flow patterns.

By coupling different instruments in Spool Pieces (suitable to be installed in industrial facilities) and by the development of models for the instruments, the mass flow rate of the two phases for different flow conditions has be estimated. The proposed methods allow the possibility to measure the mass flow rate of the phases by using three, two or one instruments with different degree of accuracy.

Advantage and drawbacks of the different instrument combinations have been highlighted, and the accuracy achievable for each SP configuration has been estimated. Moreover the experimental analysis performed with the different instruments, at different flow conditions and geometrical configurations, has allowed the investigation and the characterization of the air-water flow in a wide range of flow patterns, and new correlations able to estimate two-phase flow parameters, such as void fraction and two-phase flow pressure drops, have been found.

Future work will be addressed to investigate the performance of the different SP in transient conditions with fixed periodic oscillations. Tests with a SP consisting of a venturi flow meter and a an Electrical Capacitance Probe in horizontal flow across 80 mm diameter pipes are being carried out too.

Ackowledgements

The present research activity has been supported by ENEA and by the Ministry of Economic Development. A special thanks to R. Costantino and G. Vannelli for their support in the laboratory.

Nomenclature

C VFM discharge coefficient
C^* normalized electrical capacitance
F signal acquisition frequency

J superficial velocity
Re Reynolds number
V* WMS normalized signal
W mass flow rate
x flow quality
α void fraction
Δp differential pressure
ρ density
Φ two- phase multiplier
χ Martinelli parameter

Subscripts
g gas
i WMS i-th vertical index
irr irreversible
j WMS j-th horizontal index
k WMS time index
l liquid
TP Two-Phase

References

[1] Carelli M D, Conway L E, Oriani L, Petrović B, Lombardi C V, Ricotti M E, Barroso A C O, Collado J M, Cinotti L, Todreas N E, Grgić D, Moraes M M, Boroughs R D, Ninokata H, Ingersoll D T, Oriolo F, The Design and Safety Features of the IRIS Reactor, *Nucl. Eng. Design*, 230, pp. 151-167 (2004).

[2] Bertani C, De Salve M, Malandrone M, Monni G, Panella B, State-of-Art and selection of techniques in multiphase flow measurement, Report RdS/2010/67 ENEA (2010).

[3] De Salve M, Monni G, Panella B, Turbine Flow Meter and Drag-Disk in Horizontal Air Water Flow. , In: UIT2011, Torino (Italia), 20-22 Giugno 2011. pp. 107-112, (2011)

[4] De Salve M, Monni G, Panella B, A Model for a Spool Piece made up of Venturi and Void fraction Flow Meter in Horizontal Flow, In: *ANS TRANS.*, vol. 108 , pp. 1013-1016. - ISSN 0003-018X (2013).

[5] De Salve M, Monni G, Panella B, Horizontal Air-Water Flow Analysis with Wire Mesh Sensor. In: JoP, vol. 395, 012179-. - ISSN 1742-6588 (2012).

[6] Monni G, De Salve M, Panella B, Randaccio C, Electrical Capacitance Probe Characterization in Vertical Annular Two-Phase Flow. In: *SCI TECHNOL NUCL INSTAL*, vol. 2013, Article ID 568287, pp. 1-12. - ISSN 1687-6075 (2013).

[7] Monni G, PhD Thesis, Politecnico di Torino, (2014).

[8] Prasser H M, Krepper E, Lucas D, Evolution of the two-phase flow in a vertical tube-decomposition of gas fraction profiles according to bubble size classes using wire-mesh sensors, *Int. J. Therm. Sci*., 41 17–28 (2002).

[9] Prasser H M, Böttger A, Zschau J, A new electrode-mesh tomograph for gas–liquid flows, *Flow Measurement and Instrumentation*, 1998, 9 111–9 (1998).

[10] Pietruske H, Prasser H M, Wire-mesh sensors for high-resolving two-phase flow studies at high pressures and temperatures, *Flow Measurement and Instrumentation*, 2007 18 87-94 (2007).

[11] Teletronic Rossendorf GmbH, Wire Mesh Sensor System, WMS200 Manual, Version 1.2, December 9, 2010

[12] De Salve M, Monni G, Panella B, Horizontal Two-Phase Flow Pattern Recognition, presented at 8th World Conf. on Exp. Heat Transfer, Fluid Mech., and Thermodyn., Lisbon, Portugal, June 16-20 (2013), *Exp. Therm. Fluid Sc*., in print.

[13] Averill and Goodrich, Design and performance of a drag Disc and Turbine transducer. For LOFT Experimental Program, (1979).

[14] Aya I, A model to calculate mass flow rate and other quantities of two-phase flow in a pipe with densitometer , a drag disk and a turbine meter, ORNL-TM-4759 (1975).

[15] De Salve M, Monni G, Panella B. Analisi delle prestazioni di uno *Spool Piece* in deflusso orizzontale bifase aria-acqua . SPOOL PIECE costituto da TURBINA e DRAG DISK, Report ENEA, Luglio (2011).

[16] Baker C R, Flow Measurement Handbook, Cambridge University Press (2000).

[17] Lockhart R W and Martinelli R C, Proposed correlation of data for isothermal two- phase two-component flow in pipe, *Chem. Eng. Prog*. 45 39-48 (1949).

[18] Baroczy C J, A systematic correlation for two-phase pressure drop, AIChE reprint 37 presented at 8th National Heat Transfer Conference, Los Angeles, (1965).

[19] Chisholm D and Rooney D H 1974 Research note: Two-phase flow through sharp-edged orifices, *J Mech. Eng. Sci.* 16 353-55 (1962).

[20] Wallis G B, One-Dimensional Two-Phase Flow, McGraw Hill, 2nd Edition, New York, 1979.

[21] Achilli A, Greco M, Progettazione di una sonda capacitiva per misurazione del grado di vuoto medio di sezione di miscele bifase acqua-vapore, Report RdS/2010/x ENEA (2010).

[22] De Salve M, Monni G, Panella B, Caratterizzazione di una Sonda capacitiva in deflusso verticale ascendente aria-acqua Report RdS/2011/121

[23] Monni G, De Salve M, Panella B, Randaccio C, Electrical Capacitance Probe Characterization for Vertical Annular air-water Flow, in 9th International Conference on Heat Transfer, *Fluid Mechanics and Thermodynamics*, July 2012 Malta (2012).

[24] Ishii M, Mishima K, Two-fluid model and Hydrodynamic constitutive relations, *Nuclear Engineering and Design*, Vol. 82, pp. 107-126 (1984).

[25] Ferri R, Congiu C, SPES3-IRIS facility RELAP5 base case transient analyses for design support, SIET document 01 489 RT 09 Rev.0 (2009).

[26] De Salve M, Monni G, Panella B, A Model for a Spool Piece made up of Venturi and Void fraction Flow Meter in Horizontal Flow, *Trans. ANS*, Vol. 108 1013-1016, Atlanta, Georgia, June 16–20 (2013).

[27] Lockhart R W and Martinelli R C, Proposed correlation of data for isothermal two- phase two-component flow in pipe *Chem. Eng. Prog.* 45 39-48 (1949).

[28] Chisholm D, Two-phase flow through sharp edged orifices. *J. Mech. Eng. Sci*., 19(3), 128–30 (1977).

[29] Murdock J W, Two-phase Flow Measurement with Orifices, *ASME J. Basic Eng*., December, 419-433 (1962).

[30] Zhang H J, Yue W T, Huang Z Y, Investigation of oil–air two-phase mass flow rate measurement using venturi and void fraction sensor, J. Zhejiang University Science 6A (6) (2005).